

Effect of bis-(3-sodiumsulfopropyl disulfide) byproducts on copper defects after chemical mechanical polishing

Chi-Cheng Hung, Wen-Hsi Lee, Shao-Yu Hu, Shih-Chieh Chang, Kei-Wei Chen, and Ying-Lang Wang

Citation: *Journal of Vacuum Science & Technology B* **26**, 255 (2008); doi: 10.1116/1.2834679

View online: <http://dx.doi.org/10.1116/1.2834679>

View Table of Contents: <http://scitation.aip.org/content/avs/journal/jvstb/26/1?ver=pdfcov>

Published by the AVS: Science & Technology of Materials, Interfaces, and Processing

Articles you may be interested in

[Effect of temperature on copper damascene chemical mechanical polishing process](#)

J. Vac. Sci. Technol. B **26**, 141 (2008); 10.1116/1.2825143

[Development of chemical-mechanical polished high-resolution zone plates](#)

J. Vac. Sci. Technol. B **25**, 1789 (2007); 10.1116/1.2790917

[Multivariable control of multizone chemical mechanical polishing](#)


J. Vac. Sci. Technol. B **22**, 1679 (2004); 10.1116/1.1761483

[Electrochemical behavior of copper chemical mechanical polishing in KIO₃ slurry](#)





J. Vac. Sci. Technol. B **20**, 608 (2002); 10.1116/1.1458956

[Investigations of effects of bias polarization and chemical parameters on morphology and filling capability of 130 nm damascene electroplated copper](#)

J. Vac. Sci. Technol. B **19**, 767 (2001); 10.1116/1.1368673



Instruments for Advanced Science

<p>Contact Hiden Analytical for further details: W www.HidenAnalytical.com E info@hiden.co.uk</p> <p>CLICK TO VIEW our product catalogue</p>	 <p>Gas Analysis</p> <ul style="list-style-type: none"> › dynamic measurement of reaction gas streams › catalysis and thermal analysis › molecular beam studies › dissolved species probes › fermentation, environmental and ecological studies 	 <p>Surface Science</p> <ul style="list-style-type: none"> › UHV TPD › SIMS › end point detection in ion beam etch › elemental imaging - surface mapping 	 <p>Plasma Diagnostics</p> <ul style="list-style-type: none"> › plasma source characterization › etch and deposition process reaction › kinetic studies › analysis of neutral and radical species 	 <p>Vacuum Analysis</p> <ul style="list-style-type: none"> › partial pressure measurement and control of process gases › reactive sputter process control › vacuum diagnostics › vacuum coating process monitoring
---	--	--	--	--

Effect of bis-(3-sodiumsulfopropyl disulfide) byproducts on copper defects after chemical mechanical polishing

Chi-Cheng Hung, Wen-Hsi Lee, and Shao-Yu Hu

Department of Electrical Engineering, National Cheng Kung University, Tainan 701, Taiwan, R.O.C.

Shih-Chieh Chang, Kei-Wei Chen, and Ying-Lang Wang^{a)}

Department of Applied Physics, National Chiayi University, Chiayi, Taiwan, R.O.C.

and Department of Material Science, National University of Tainan, Taiwan, R.O.C.

(Received 3 August 2007; accepted 19 December 2007; published 28 January 2008)

In the semiconductor metallization process, the superior gap-fill capability of copper (Cu) electroplating is mainly due to external additives, such as bis-(3-sodiumsulfopropyl disulfide) (SPS), which is used as an accelerator. This study demonstrates that the byproducts of SPS induced Cu defects after a chemical-mechanical-polishing (CMP) process. In conventional cyclic-voltammetric-stripping analysis, the byproducts generated from organic additives are very difficult to quantify. In this study, the authors used mass-spectrum analysis to quantify SPS byproducts and found that the SPS byproduct, 1,3-propanedisulfonic acid, correlated with the formation of Cu defects because it influenced the properties of electroplated Cu films and the chemical corrosion rate, then induced defects after the CMP process. © 2008 American Vacuum Society. [DOI: 10.1116/1.2834679]

I. INTRODUCTION

In semiconductor device manufacturing, electroplating is the main technology used to form fine Cu interconnects due to its excellent gap-fill capability.¹⁻⁹ The superior gap-fill capability of Cu electroplating is mainly due to external additives, such as bis-(3-sodiumsulfopropyl disulfide) (SPS) used as an accelerator or polyalkylene glycol (PAG) used as a suppressor. In prior literature, the function of organic additives has been widely discussed. Moffat *et al.* proposed the kinetics of Cu electroplating in a cupric-sulfate electrolyte containing SPS-polyethylene glycol (PEG)-Cl.³⁻⁶ Kelly and West demonstrated that PEG inhibited the Cu-electroplating rate in the presence of Cl⁻.^{8,9}

Chemical mechanical polishing (CMP) is the most promising way to remove overburdened metals to realize planarization in the damascene metallization process.¹⁰⁻¹⁸ Conventional CMP slurries usually contain strong oxidizers and hard abrasives, easily leading to the formation of various defects on Cu metals. Typically, Cu defects are caused by Cu corrosion, including chemical corrosion, galvanic corrosion, and photocorrosion during the CMP process.¹⁰⁻¹⁴ On the other hand, when a plating bath is used continuously, the organic additives within the plating bath will break down to more byproducts that will induce defect formation.

In commercial electroplating processes, the concentration of organic additives is monitored by a cyclic-voltammetric-stripping (CVS) method. This is an accurate and precise method for controlling the electroplating rate, which receives contributions from all the additives in the plating bath. However, the CVS method is not able to distinguish the effect of byproducts in the plating bath. In this study, we used a mass-

spectrum method to monitor the plating solution and quantify the byproducts of SPS. Among all the SPS oxidized byproducts, 1,3-propanedisulfonic acid (PDS) is the most stable one. The effect of PDS on the quality of electroplated Cu films was investigated in this study. In addition, the corrosion behavior of Cu films deposited in the plating bath containing different PDS concentrations was examined by electrochemical impedance spectroscopy. An equivalent circuit was also proposed to realize the effect of PDS on the Cu corrosion.

II. EXPERIMENTAL DETAILS

All experimental wafers were composed of a 30-nm-thick ionized-metal-plasma (IMP)-Ta/TaN_x layer as a diffusion barrier and a 200-nm-thick IMP-Cu film as a seed layer. A Cu-electroplating bath included cupric sulfate, sulfuric acid, chloride ions, PAG and/or SPS. A film was deposited under galvanostatic control at room temperature and the plating current density was 10 mA/cm². After Cu electroplating, the Cu films were annealed at 180 °C for 30 s. Potentiodynamic (PD) polarization and electrochemical impedance spectroscopy were carried out in a three-electrode cell using a computer-controlled Princeton Applied Research PARSTATTM 2273. The counter electrode was platinum and the working electrode was a rotating Cu disk electrode constructed from a 0.5 cm² rod of 99.999% pure Cu embedded in nonconductive, non-reactive epoxy. All potentials were reported relative to a Ag/AgCl electrode, which was used as the reference electrode.

The stress of Cu film was measured by a KLA-Tencor FX100 unit. The circuit of the electrochemical system was built, and the values of the elements in this circuit were simulated using ZSimpWin version 3.1 software. In addition, the defects on Cu films were scanned by KLA-Tencor Surf-

^{a)} Author to whom correspondence should be addressed: Department of Material Science, National University of Tainan, Taiwan, R.O.C.; electronic mail: ylwang@tsmc.com

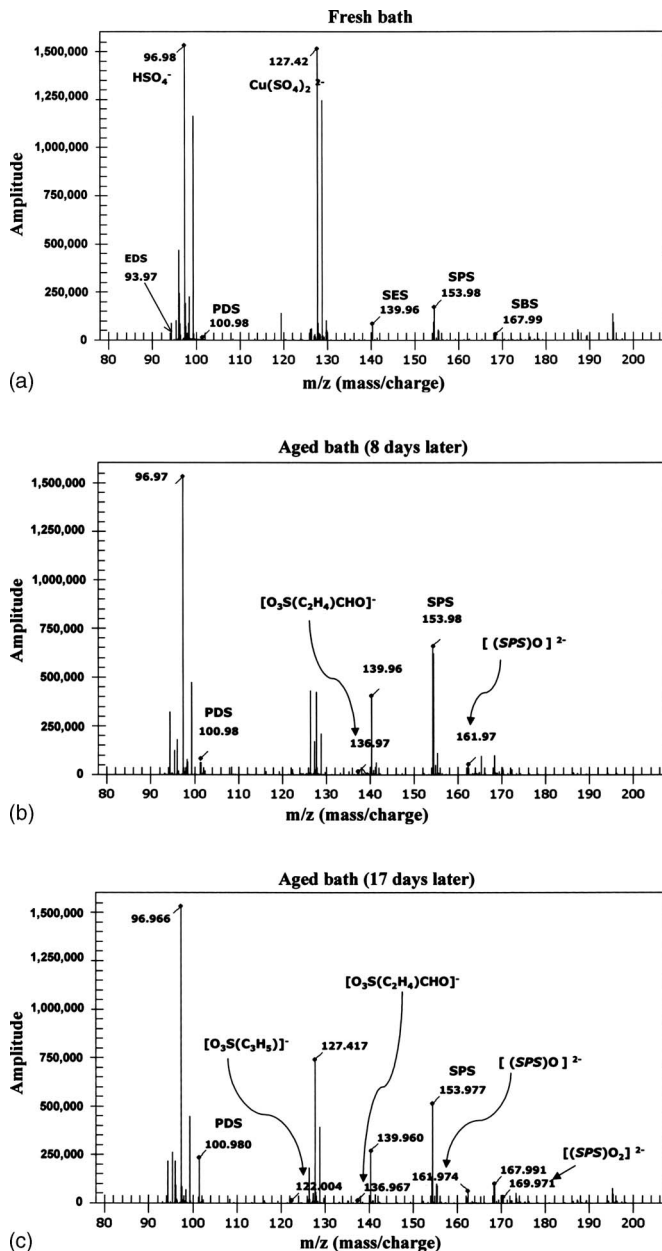


FIG. 1. Mass spectrum of (a) fresh plating bath, (b) aged plating bath with 8 day idle time, and (c) aged plating bath with 17 day idle time.

scan SP1 MX and then reviewed using the scanning electron microscope (SEM) of the KLA-Tencor SEMVision unit. All organic additives were measured using mass-spectrometry based on a Metara Sentry CCM™ tool.

III. RESULTS AND DISCUSSION

In the Cu-electroplating process, the accelerator, SPS, plays an important role in the gap-fill capability. However, SPS species easily oxidize and break down in an acidic plating bath, particularly after a long bath idle-time in the presence of a Cu anode. The chemical reactions of SPS oxidation in an acidic plating bath include many pathways. One pathway [Eqs. (1)–(3)] is the direct oxidation of the SPS species and oxygen atom, then the formation of $\text{SPS}(\text{O}_2)^{2-}$ further

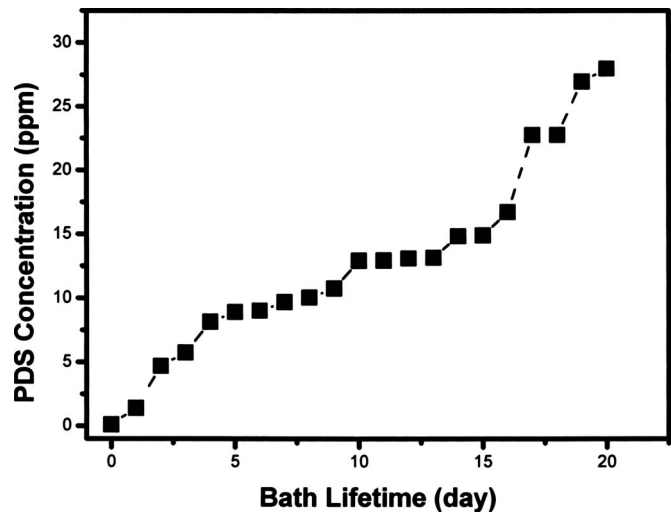
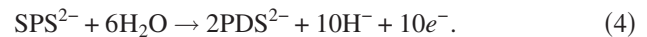
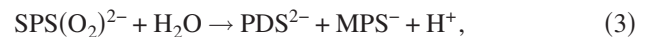
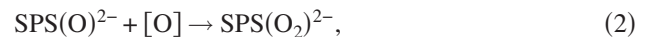


FIG. 2. Relationship between the concentration of PDS and go-through time of plating bath.

hydrolyzes to generate PDS and 3-mercaptopropanesulfonic acid (MPS). The other pathway [Eq.(4)] is that SPS directly hydrolyzes to form PDS:



Among all of the SPS oxidized byproducts, PDS is the most stable one, having a concentration increase with increasing bath idle-time or amount of wafer running. PDS easily accumulates in the plating bath. Hence, in the study, we used a mass-spectrometry method to calculate the PDS concentration. Figure 1(a) shows the mass spectrum of a fresh bath.

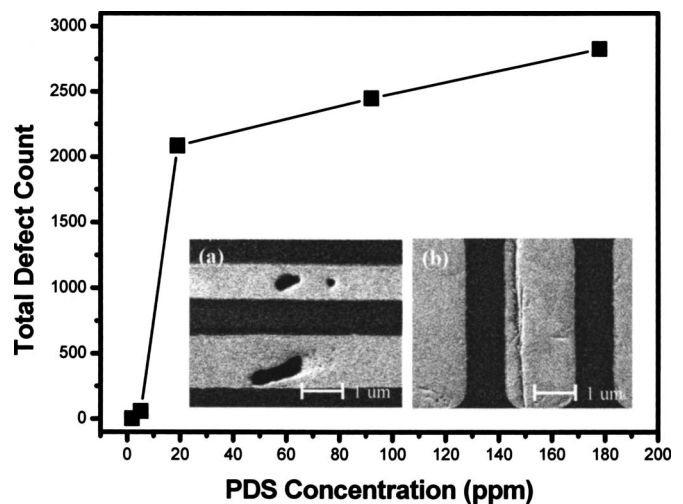


FIG. 3. Total defects on Cu metals in relation to the concentration (0–180 ppm) of PDS. The inset shows the SEM top-view images of (a) void defect and (b) scratch defect on Cu lines.

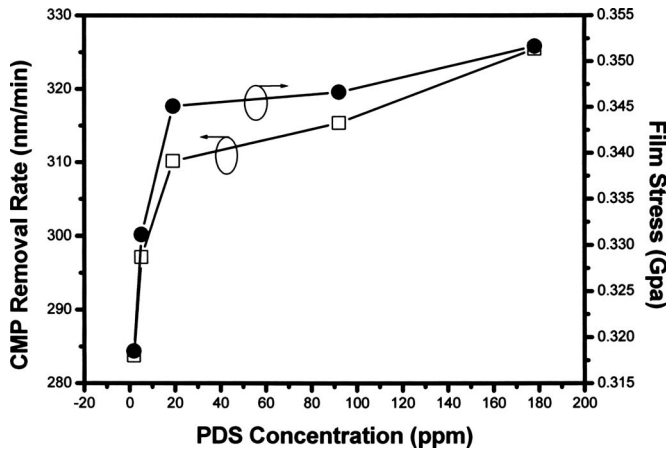


FIG. 4. Effect of the PDS concentration on the stress and CMP removal rate of electroplated Cu films.

The concentrations of PDS and SPS were quantified by the spikes of 1,3-ethanedisulfonic acid (EDS), bis(2-sulfethyl) disulfide (SES), and bis(1-sulfopropyl-1-sulfobutyl) disulfide (SBS). Sequentially, the spectra of an aged bath and the byproducts of SPS are shown in Figs. 1(b) and 1(c). From the spectra, the peak of the PDS species is obviously higher and the concentration of PDS increases with the bath idle-time. Figure 2 shows that the PDS concentration increases from 0 to ~ 30 ppm as the bath idle-time increases from 0 to 20 days. Figure 3 reveals that the total counts of Cu defects after the CMP process increase with increasing PDS concentration. Long narrow strip defects such as scraping on the Cu surface are defined as scratch defects, and hollow hole defects such as removing a lump of Cu are defined as void defects. The SEM images show that the Cu defects include scratches and voids, as shown in the inset of Fig. 3. When the PDS concentration is more than 20 ppm, the Cu films are seriously damaged by the CMP process. Figure 4 also shows

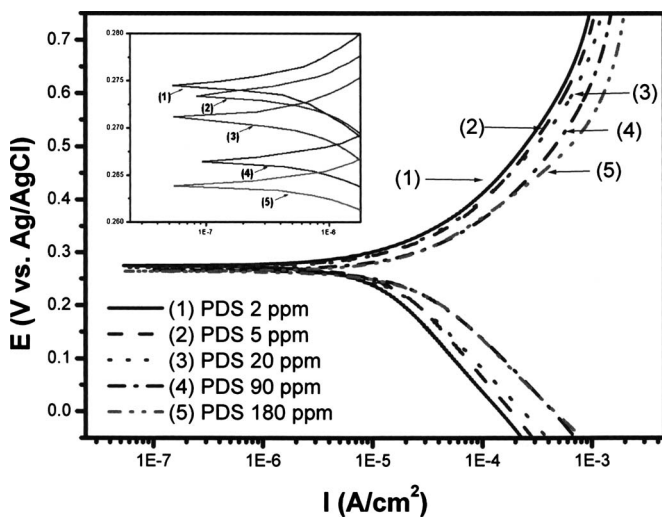
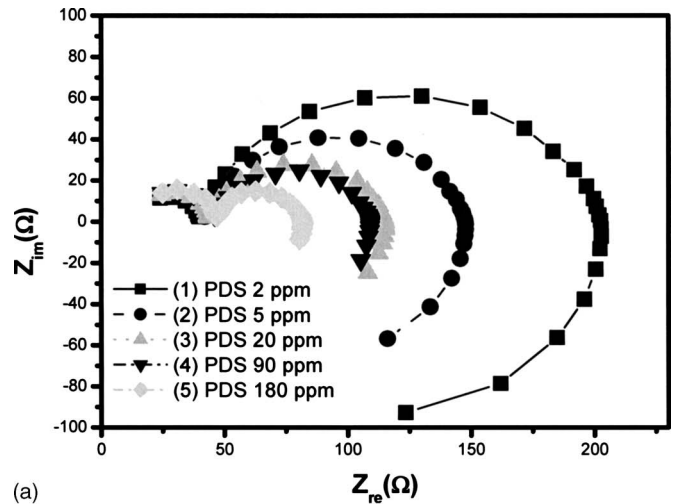
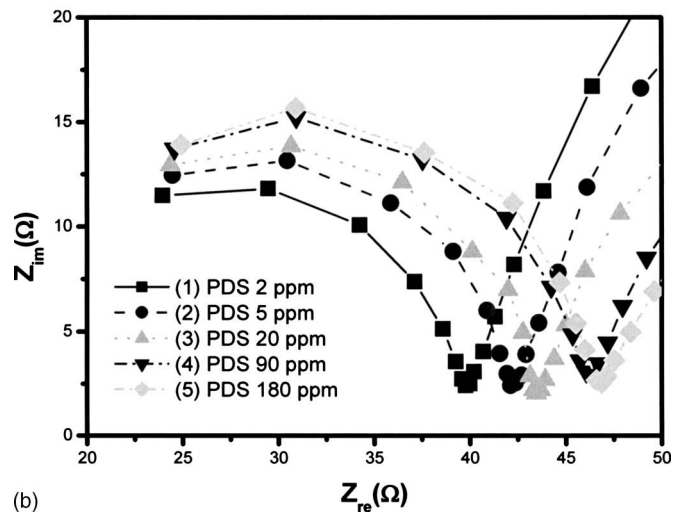


FIG. 5. PD polarization curves of electroplated Cu films deposited in the plating bath containing the PDS concentration of (1) 2 ppm, (2) 5 ppm, (3) 20 ppm, (4) 90 ppm, and (5) 180 ppm; the inset is a magnification of the position of OCP.



(a)



(b)

FIG. 6. (a) Nyquist plots of electroplated Cu films deposited in the plating bath containing the PDS concentration of (1) 2 ppm, (2) 5 ppm, (3) 20 ppm, (4) 90 ppm, and (5) 180 ppm; (b) is a magnification of impedance close to zero at the high-frequency region. Z_{im} is the imaginary resistance and Z_{re} is the real resistance.

that the stress of Cu films becomes more tensile as the PDS concentration of plating baths increases. Moreover, the CMP removal rate increases with increasing film tensile stress. In the Cu-electroplating process, we found that the stress of Cu films is a key factor in inducing Cu defects. In the CMP process, Cu metals are corroded and oxidized by slurry chemicals. The proposed mechanism is that the bonding strength between Cu atoms is weakened as the tensile stress increases, leading to Cu metals that are easily corroded and removed by the slurry chemicals. A similar result was demonstrated in a Cu-electropolishing process.¹⁵ In addition, the PD polarization curves show that the Cu films electroplated from a bath with higher PDS concentration have a larger corrosion current in the CMP slurry, as seen in Fig. 5. At the same time, increasing the PDS concentration decreases the open-circuit potential (OCP), indicating that the Cu films are easily corroded in the CMP slurry, as shown in the inset of Fig. 5.¹⁶ The result is consistent with the data of Fig. 4. In the

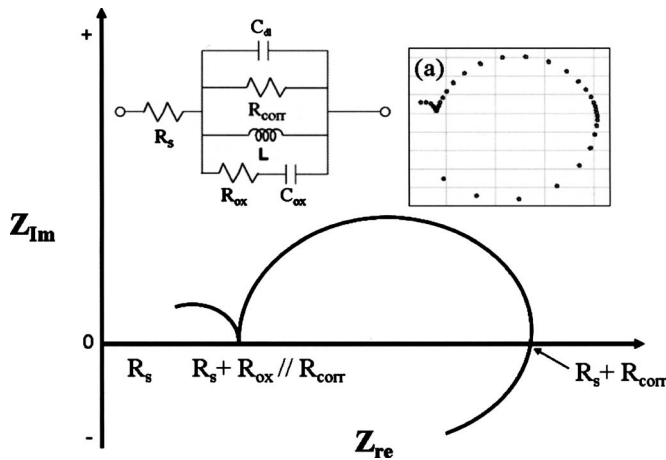
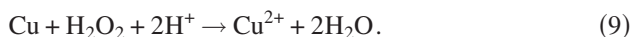
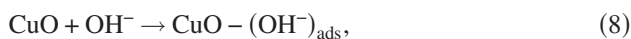
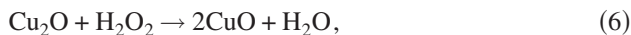
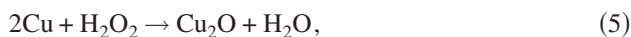


FIG. 7. Proposed equivalent-circuit diagram of Cu corrosion in the CMP slurry. Chart (a) is a simulation map. The Z_{re} is equal to $R_s + R_{ox} // R_{corr}$ due to C_{dl}/L open and C_{ox} short in a special frequency (~ 36 kHz).

impedance analysis, the Nyquist plots of the Cu electrochemical system in the CMP slurries indicate that the semi-circle becomes smaller as the PDS concentration increases, as shown in Fig. 6(a). On the contrary, Fig. 6(b) shows that the Z_{im}/Z_{re} ratio, where Z_{im} is the imaginary resistance and Z_{re} is the real resistance, increases with increasing PDS concentration. Figure 7 shows the simulated equivalent circuit of the Cu electrochemical system, where the chart (a) inserted in Fig. 7 clarifies the exact configuration of the circuit. In addition, the chemical reactions of Cu metals in CMP slurries occur through the following steps:^{17,18}



After simulation, there are three resistances, two capacitances, and one inductance in this electrochemical system, where R_s is the bulk-solution resistance, C_{dl} is the double-layer capacitance, C_{ox} is the oxidation-layer capacitance, R_{ox} is the resistance of Cu oxides for reactions (5)–(8), R_{corr}

is the charge-transfer resistance (associated with the double layer) for reaction (9), and L is the adsorption-layer inductance for reactions (5)–(8). In the CMP process, the Cu films are oxidized by hydrogen peroxide and react with OH^- ions to adsorb on the Cu surface.¹⁸ Therefore, the thin Cu oxides formed on the Cu surface to cause capacitance effects (C_{ox}) and the interface between Cu films and CMP slurries also formed the capacitance effects of double layers (C_{dl}) due to Cu ions separating and accumulating. The values of the circuit's components in Fig. 7 are obtained by fitting the Nyquist spectra of Fig. 6(a) and are summarized in Table I. C_{ox} is represented as a constant-phase element (CPE) and can be calculated from Eq. (10):

$$C_{ox} = \frac{(Y_{ox} \times R_{ox})^{(1/\alpha_{ox})}}{R_{ox}}, \quad (10)$$

where Y_{ox} is the admittance and α_{ox} is defined as the phase angle of the CPE impedance independent of the frequency and has a value of $-(90 \times \alpha_{ox})$ deg. Consequently, the C_{ox} value of the oxidation layers decreases from 4.948 to 2.239 μF as the PDS concentration of the plating bath increases from 2 to 180 ppm. The relationship between the Cu-oxide capacitance, C_{ox} , and the Cu-oxide thickness, d , is shown in Eq. (11):

$$C_{ox} = \epsilon_0 \epsilon \frac{S}{d}, \quad (11)$$

where ϵ_0 is the permittivity of free space (8.85×10^{-12} F/m), ϵ is the dielectric constant of the Cu-oxide film (18.1), S is the surface area of Cu films (4 cm^2), and d is the film thickness. As the PDC concentration increases, the Cu-oxide thickness increases from 12.95 to 28.63 nm, resulting in an increase in the R_{ox} value. On the other hand, the value of R_{corr} decreases with increasing PDS concentration due to the larger tensile stress of electroplated Cu films. At the same time, the Cu films are more corroded and produce more cupric ions to speed the adsorption of $\text{Cu}(\text{OH})_2$; then the ions significantly influence current variation and affect inductance. The circuit of Cu corrosion in the CMP slurries can reasonably explain the overall complex chemical reactions and can also help us understand why Cu defects are produced after the CMP process.

TABLE I. Element values of equivalent circuit in Fig. 7 required for the best fitting of impedance spectra in Fig. 6(a).

PDS (ppm)	R_s/Ω	R_{ox}/Ω	CPE _{ox}		$C_{ox}/\mu\text{F}$	R_{corr}/Ω	C_{dl}/nF	L
			$Y_{ox}/(\mu\Omega^{-1})$	α_{ox}				
2	15.54	27.57	24.73	0.8192	4.948	188.2	8.998	0.3688
5	15.33	33.54	17.36	0.8401	4.206	132.8	8.329	0.4034
20	15.52	38.64	15.81	0.8347	3.651	99.81	8.445	0.4621
90	15.78	44.58	10.88	0.8395	2.529	93.39	8.321	0.5805
180	15.66	48.13	10.37	0.8322	2.239	66.09	8.348	0.6247

IV. CONCLUSION

In a conventional CVS analysis, the byproducts broken down from organic additives are very difficult to quantify. In this study, we used a mass-spectrum analysis to quantify the byproducts of SPS. We found that PDS is the most stable SPS byproduct. Increasing the PDS concentration will increase the tensile stress of Cu films. From the simulated results, we know that the oxidation rate and corrosion rate of electroplated Cu films will be enhanced as the PDS concentration of plating baths increases, inducing more defect formation after the Cu-CMP process.

ACKNOWLEDGMENT

This work was supported by the National Science Council of Taiwan. (Grant No. NSC 96-221-E-006-125 and NSC 97-2623-7-006-012-ET.) The authors are thankful for the technical support from the National Cheng Kung University, Tainan, Taiwan.

¹P. C. Andricacos, C. Uzoh, J. O. Dukovic, J. Horkans, and H. Deligianni, *IBM J. Res. Dev.* **42**, 567 (1998).

²D. Edelstein, J. Heidenreich, R. Goldblatt, W. Cote, C. Uzoh, N. Lustig, P. Roper, T. McDevitt, W. Motsiff, A. Simon, J. Dukovic, R. Wachnik, H. Rathore, R. Schulz, L. Su, S. Luce, and J. Slattery, *Technical Digest, IEEE International Electron Devices Meeting* (1997), p. 773.

³T. P. Moffat, J. E. Bonevich, W. H. Huber, A. Stanishevsky, D. R. Kelly, G. R. Stafford, and D. Josell, *J. Electrochem. Soc.* **147**, 4524 (2000).

⁴D. Josell, D. Wheeler, W. H. Huber, and T. P. Moffat, *Phys. Rev. Lett.* **87**, 016102 (2001).

⁵D. Josell, D. Wheeler, and T. P. Moffat, *Electrochem. Solid-State Lett.* **5**, C49 (2002).

⁶T. P. Moffat, D. Wheeler, W. H. Huber, and D. Josell, *Electrochem. Solid-State Lett.* **4**, C26 (2001).

⁷S. Y. Chiu, J. M. Shieh, S. C. Chang, K. C. Lin, B. T. Dai, C. F. Chen, and M. S. Feng, *J. Vac. Sci. Technol. B* **18**, 2835 (2000).

⁸J. J. Kelly and A. C. West, *J. Electrochem. Soc.* **145**, 3472 (1998).

⁹J. J. Kelly and A. C. West, *J. Electrochem. Soc.* **145**, 3477 (1998).

¹⁰K. W. Chen, Y. L. Wang, L. Chang, S. C. Chang, F. Y. Li, and S. H. Lin, *Electrochem. Solid-State Lett.* **7**, G238 (2004).

¹¹A. Beverina, H. Bernard, J. Palleau, J. Torres, and F. Tardif, *Electrochem. Solid-State Lett.* **3**, 156 (1999).

¹²Y. Homma, S. Kondo, N. Sakuma, K. Hinode, J. Noguchi, N. Ohashi, H. Yamaguchi, and N. Owada, *J. Electrochem. Soc.* **147**, 1193 (2000).

¹³S. Kondo, N. Sakuma, Y. Homma, and N. Ohashi, *Jpn. J. Appl. Phys., Part 1* **39**, 6216 (2000).

¹⁴D. Ernur, S. Kondo, D. Shamiryan, and K. Maex, *Microelectron. Eng.* **64**, 117 (2002).

¹⁵S. C. Chang, J. M. Shieh, J. Y. Fang, Y. L. Wang, B. T. Dai, and M. S. Feng, *J. Vac. Sci. Technol. B* **22**, 116 (2004).

¹⁶M. Kodera, S. I. Uekusa, H. Nagano, K. Tokushige, S. Shima, A. Fukunaga, Y. Mochizuki, A. Fukuda, H. Hiyama, M. Tsujimura, H. Nagai, and K. Maekawa, *J. Electrochem. Soc.* **152**, G506 (2005).

¹⁷V. R. K. Gorantla, K. A. Assiongbon, S. V. Babu, and D. Roy, *J. Electrochem. Soc.* **152**, G404 (2005).

¹⁸J. Y. Lin, C. C. Wan, Y. Y. Wang, J. C. Chen, J. Y. Lai, Y. D. Fan, and J. P. Chuang, *J. Electrochem. Soc.* **154**, H530 (2007).